Electronic structure of cation-deficient CoO from first principles

U. D. Wdowik* and K. Parlinski
Institute of Technology, Pedagogical University, ulica Podchorazych 2, PL-30-084 Cracow, Poland
(Received 19 August 2007; revised manuscript received 30 December 2007; published 7 March 2008)

Generalized gradient approximation with correction for Hubbard energy was used to study electronic and magnetic properties of defected CoO. Vacancies were introduced into the cobalt sublattice. Calculations were performed for point defect concentrations of 3.125% and 6.25%. Trivalent cobalt ions are created in both ferromagnetic cobalt sublattices, inducing acceptor states located in the band gap of the CoO matrix. They arise from a charge transfer which converts initial divalent cobalt to trivalent state. Concentration of trivalent cobalts is twice as large as the concentration of cation vacancies. Our *ab initio* calculations support experimental data obtained previously by emission Mössbauer spectroscopy.

DOI: 10.1103/PhysRevB.77.115110 PACS number(s): 61.72.J−, 71.15.Mb, 74.62.Dh, 75.50.Ee

I. INTRODUCTION

The family of transition-metal oxides comprises an important class of materials exhibiting a variety of electronic, optical, and magnetic properties which make these oxides suitable for a basis of a new type of electronics.[1–3] Moreover, the physics of these compounds is very often governed by the strong electron correlations, which makes these materials very interesting from the fundamental point of view.

Electronic structure and magnetic properties of 3*d* transition-metal oxides (NiO, CoO, FeO, and MnO) have been extensively studied by *ab initio* methods; however, most of these investigations were focused on pure systems.[4–7] Recently, Ködderitzsch *et al.*[8] performed first principles calculations for defected NiO and MnO crystals and found a vacancy-induced half-metallicity of these compounds.

Paramagnetic CoO is a nonstoichiometric *p*-type semiconductor with a band gap of approximately 2.8 eV.[9,10] It crystallizes in a cubic rocksalt structure (space group $Fm\bar{3}m$) with a lattice parameter of 4.26 Å.[11,12] The nonstoichiometry is mainly due to cobalt vacancies and it depends on temperature and oxygen pressure. It increases both with increasing temperature and oxygen pressure. There are practically no Co interstitials, and the oxygen sublattice is almost perfectly ordered.[13] The concentration of cobalt vacancies lies in the range 0.1%–3%.[14] Vacancies are believed to stay either in uncharged or charged states.[15] Uncharged Co vacancies are accompanied by trivalent cobalt ions. Therefore, a defect band can be composed of Co^{3+} ions, uncharged Co vacancies, and singly and doubly charged cobalt vacancies. Uncharged vacancies are able to accept up to two electrons. Trivalent cobalt ions and uncharged vacancies are acceptors, doubly charged vacancies are donors, while singly charged vacancies can be either acceptors or donors.[16]

At low temperature, CoO adopts a distorted NaCl structure.[17] A small tetragonal distortion ($c/a=0.988$) is accompanied by a rhombohedral distortion (the angle of the pseudocubic cell amounts to 89.962°), the latter being due to antiferromagnetic ordering of cobalt moments along ⟨111⟩ direction.[18–20] A second kind of antiferromagnetic ordering (AFII) is realized below the Néel temperature (about 293 K). In the AFII arrangement, the magnetic moments of transition-metal ions are parallel within (111) planes and they are antiparallel to each other between the adjacent (111) planes. Therefore, the majority and minority spins in alternating (111) planes form two ferromagnetic sublattices. The AFII supercell is twice as large as the crystallographic unit cell and the symmetry of the lattice is consistent with that of the magnetic structure.

Computational methods based on density functional theory (DFT) and employing the local density approximation (LDA) or generalized gradient approximation (GGA) with corrections for strong on-site Coulomb interactions (LDA $+U$ or GGA$+U$) could predict correct ground states of CoO (Ref. 4) and indicated that this system is a charge-transfer insulator.[21]

The present paper deals with the influence of point defects such as cationic vacancies on the electronic structure of charge-transfer insulator, CoO. Electron correlations are taken into account via the Hubbard potential U and the exchange interaction parameter J. Calculations are compared with the results of emission Mössbauer spectroscopy. It is shown that trivalent states of cations in CoO matrix arise directly from the charge-transfer process.

II. COMPUTATIONAL DETAILS

A. Method

The calculations have been performed within the spin-polarized DFT implemented in Vienna *ab initio* simulation package.[22] Atoms were represented by projector-augmented wave pseudopotentials.[23] The valence electrons of cobalt and oxygen were described by the potential configurations ($3d^8 4s^1$) and ($2s^2 2p^4$), respectively. Gradient corrected exchange-correlation functional in the form of GGA-PW91 was used[24] and a plane-wave expansion up to 520 eV was applied. Effects of electron correlation beyond GGA were taken into account within the framework of GGA$+U$ and the simplified (rotationally invariant) approach of Dudarev *et al.*[5] The Coulomb repulsion $U=7.1$ eV and the local exchange interaction $J=1$ eV were applied to describe the on-site interactions in the cobalt 3*d* shell. These values reproduce the experimental energy gap of CoO and give the spin magnetic moment on cobalt ion of $2.74\mu_B$.[25] The Brillouin

zone was sampled using $2\times2\times2$ k-point mesh generated by the Monkhorst-Pack scheme.[26] Density of states has been calculated with the $6\times6\times6$ k-point mesh and using the linear tetrahedron method with Blöchl corrections.[27] For geometry optimizations, a combination of conjugate gradient energy minimization and a quasi-Newton force minimization was used. During defect calculations, the symmetry constraints were removed, the lattice vectors of the supercell were frozen, and all atoms were allowed to relax until forces acting on atoms were less than 0.005 eV/Å. The ionic degrees of freedom were converged better than 1 meV.

B. Vacancies

A supercell approach was used to simulate the effect of introducing vacancies into the cobalt sublattice. Initial CoO structure with D_{3d}^5 ($R\bar{3}m$) symmetry contained 64 atoms which comprised 32 f.u. A neutral vacancy was created by removing one neutral cobalt atom from this 64 atom supercell. This corresponds to vacancy concentration $x=3.125\%$ in the whole crystal and leads to the nonstoichiometric oxide $Co_{0.97}O$. The defect-free CoO is the antiferromagnetic system exhibiting second kind of magnetic ordering and, hence, the spin-up and spin-down sublattices are symmetric. They are distinguished from each other only with respect to the orientation of magnetic moments. Therefore, no sublattice is preferred to introduce vacancy into and defecting the cobalt sublattice of the reversed spin direction gives the same effect. Hence, the cobalt atom located at $(\frac{1}{2},\frac{1}{2},\frac{1}{2})$ (the fractional coordinates refer to the supercell) was taken out of the CoO supercell.

The supercell with doubled vacancy concentration ($x=6.25\%$) was constructed in a similar manner, corresponding to $Co_{0.93}O$; however, in this case, each ferromagnetic cobalt sublattice was decorated with one neutral Co vacancy. Two neutral cobalt atoms residing in the CoO supercell at $(\frac{1}{2},\frac{1}{2},\frac{1}{2})$ and $(\frac{1}{2},\frac{1}{2},0)$ positions have been removed.

III. RESULTS AND DISCUSSION

A. Pure CoO

Here, we present the main results for undefected CoO.[25] The DFT+U approach with $U=7.1$ eV and $J=1$ eV leads to the rhombohedrally distorted structure of a space group D_{3d}^5 ($R\bar{3}m$). The distortion along $\langle111\rangle$ direction amounts to 0.3° and it arises naturally from the AFII symmetry of the rocksalt structure. Both the lattice constant of 4.27 Å and the energy gap of 2.77 eV agree with the experimental values. The calculated spin magnetic moment of $2.74\mu_B$ stays in agreement with other theoretical predictions.

Divalent cobalt (Co^{2+}) in a high-spin state configuration has the $3d$ states split by the exchange interaction into the majority- and minority-spin states. Additionally, the octahedral ligand field (due to surrounding oxygens) splits the $3d$ states into a triplet having t_{2g} symmetry and a doublet of e_g symmetry. Three t_{2g} and two e_g spin-up states are filled, while the spin-down t_{2g} states remain only partly occupied. Hence, the Co^{2+} electronic configuration can be written in the following way: $[(t_{2g}\uparrow)^3(e_g\uparrow)^2(t_{2g}\downarrow)^2]$. The calculated density of states (DOS) shown in Fig. 1 indicates the hybridization of Co $3d$ and O $2p$ orbitals. The highest occupied valence bands are dominated by oxygen $2p$ states with admixture of Co t_{2g} spin-down states. The lowest unoccupied conduction states are formed mainly by Co t_{2g} spin-down component. The character of the band gap is of a charge-transfer type.

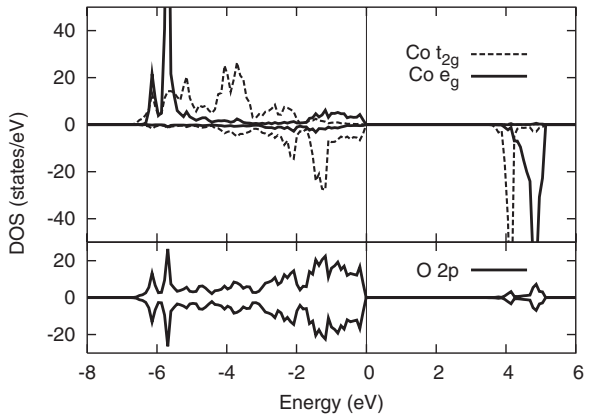

FIG. 1. Orbital projected density of states for undefected CoO. Solid and dashed curves correspond to e_g and t_{2g} projections, respectively. The positive (negative) projected densities of states represent the spin-up (spin-down) components of e_g and t_{2g} projections, respectively. The top of the valence band is taken as the reference energy. DOS is shown for spin-up cobalt sublattice.

B. Single cation vacancy

Introduction of the neutral cobalt vacancy (V_{Co}) into CoO matrix is accompanied by a very small rearrangement of neighboring atoms. The nearest oxygen ions surrounding the vacancy are displaced outward from the vacant site by about 0.12 Å. The initial Co-O distance (2.15 Å) changes by not more than 0.01 Å upon vacancy creation. There are, however, two cobalt ions for which the Co-O bond lengths are 2.05 Å. The contracted Co-O distances are observed for a cation which belongs to the next-nearest neighbors of V_{Co} and for Co ion being the most distant cation from the vacancy site. These Co ions are found as far as 2.96 and 7.41 Å from the vacancy, respectively. They differ in their charge states and magnetic moments from the rest of cations residing in $Co_{0.97}O$.

In the ionic systems, the valence charge of ions provides information about the nature of bonding between atoms in the structure and it reflects the charge-transfer processes. Therefore, we have calculated the valence charges of ions in pure and defected CoO within the Bader method.[28] Cobalt oxide has covalent-type bonds and, hence, a charge transfer between cations and anions is significantly smaller as compared to the typical ionic compounds. The calculated ionic charges for defect-free CoO are $q_{Co}=+1.33e$ and $q_O=-1.33e$. Introduction of the cobalt vacancy into the structure induces some changes in the valence charges. Figure 2 shows the dependence of the valence charges and

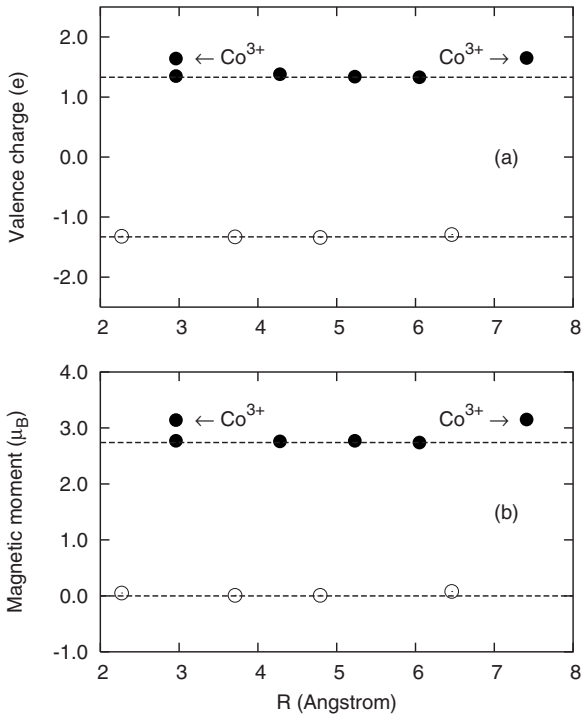

FIG. 2. Distribution of (a) valence charges and (b) magnetic moments of cations (solid symbols) and anions (open symbols) versus distance R(Å) from vacancy in $Co_{0.97}O$. The trivalent cobalts (Co^{3+}) are indicated by arrows. Dashed lines represent valence charges and magnetic moments of cations and anions in the defect-free CoO.

spin magnetic moments on the distance from the vacancy. Significant changes can be seen for these two cations which have the shortest bonds. Their valence charges increase to $+1.65e$. Simultaneously, an increase in their spin magnetic moments from the initial values of $2.74\mu_B$ to $3.15\mu_B$ is observed (Fig. 2). This indicates that an electron charge transfer takes place. The charges are transferred to oxygen p band to compensate for two holes which were created by taking one Co cation out of the insulating compound. The cobalt $3d$ states being only half filled can partly participate in a such transfer and, hence, they can become, to some extent, delocalized. Charges are transferred from cobalts to oxygens via the Co s,p states which participate in Co-O bonding. Therefore, when an electron is transferred to the oxygen band, both the valence charge and the magnetic moment of Co cation increase. Delocalization process converts initial divalent cobalt into trivalent state ($Co^{2+} \rightarrow Co^{3+} + e^-$). When a cobalt is taken out of the lattice site, nine electrons are removed from the system. Seven of them are $3d$ electrons and the remaining two are s,p electrons that have been transferred from cobalt to fill up oxygen p orbitals. Hence, two holes which are associated with the vacancy creation are compensated by two Co^{3+} ions. Trivalent cations are found in the spin-up and spin-down cationic sublattices. This allows the antiferromagnetic arrangement of cations to be retained. Electrons are transferred from the cations, which are as close as possible to their adjacent anions. On the other hand, the lattice sites occupied by Co^{3+} cations are spatially

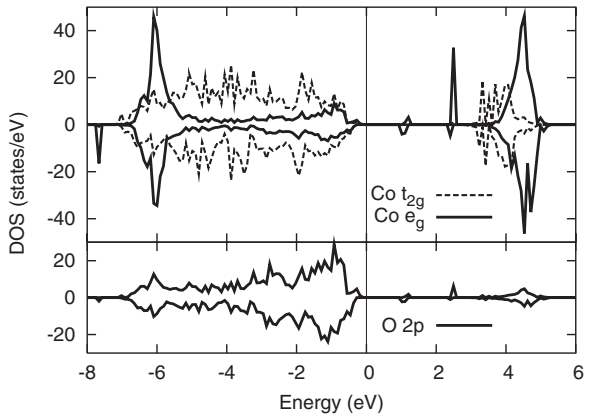

FIG. 3. Orbital projected density of states for $Co_{0.97}O$. Solid and dashed curves correspond to e_g and t_{2g} projections, respectively. The positive (negative) projected densities of states represent the spin-up (spin-down) components of e_g and t_{2g} projections, respectively. The top of the valence band is taken as the reference energy. DOS is shown for the whole cobalt sublattice.

separated and, hence, the trivalent cations can be considered as isolated ions within the cobalt sublattice.

The formation of cobalt vacancy induces additional states in the band gap. They can be seen in Fig. 3, where the calculated density of states of $Co_{0.97}O$ is shown. The narrow states inside the band gap are due to a small concentration of Co^{3+} cations. Trivalent states are located at approximately 1 eV above the valence band maximum, indicating that Co^{3+} ions act as acceptors when located in the CoO matrix. One of the previously localized $3d$ states becomes delocalized and it yields the Co^{3+} configuration. The trivalent cation e_g orbitals give the main contribution to the states residing inside the gap and they are hybridized with the oxygen $2p$ orbitals. In the $Co_{0.97}O$ structure, the oxygen $2p$ bands are spin polarized, contrary to pure CoO system where oxygen spin-up and spin-down bands are symmetric (see Fig. 1). For the ideal CoO structure with AFII ordering, oxygens are magnetically frustrated by symmetry and, hence, they do not have magnetic moments. In the CoO system with cationic vacancy, the oxygens acquire small magnetic moments since the vacancy, destroys the local symmetry. The polarized bands of an anion sublattice come from the nonequally populated spin-up and spin-down Co sublattices, which contribute different numbers of states to the total density of states. The resulting spin magnetic moment of $Co_{0.97}O$ supercell equals $2.96\mu_B$. It suggests that cobalt oxide with vacancy concentration of 3.125% is a ferromagnetic semiconductor. However, in a real defected crystal, one can find more or less distant supercell with the opposite direction of the magnetic moment. Such supercell has the cation vacancy in the cobalt sublattice with the reversed direction of magnetic moments on cations. The equal number of spin-up and spin-down ferromagnetic supercells results in the zero magnetic moment per whole crystal.

C. Double cation vacancy

One can double the concentration of cation vacancies to 6.25% by introducing an additional vacant site into the co-

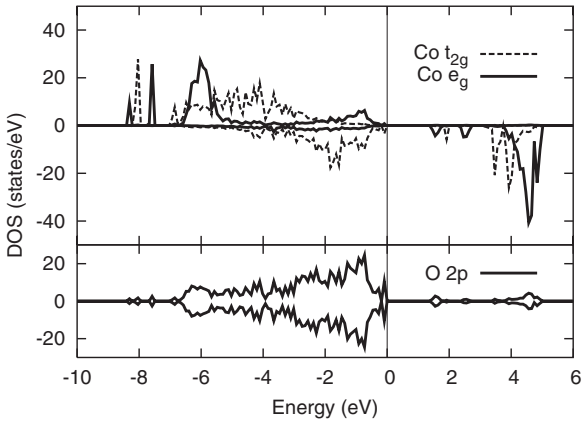

FIG. 4. Orbital projected density of states for $Co_{0.93}O$. Solid and dashed curves correspond to e_g and t_{2g} projections, respectively. The positive (negative) projected densities of states represent the spin-up (spin-down) components of e_g and t_{2g} projections, respectively. The top of the valence band is taken as the reference energy. DOS is shown for spin-up cobalt sublattice decorated with a single vacancy.

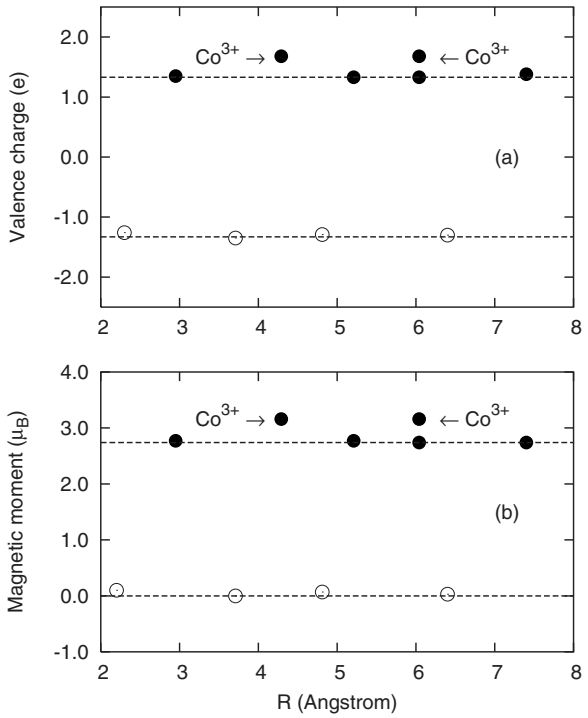

FIG. 5. Distribution of (a) valence charges and (b) magnetic moments of cations (solid symbols) and anions (open symbols) versus distance R(Å) from vacancy in $Co_{0.93}O$. The trivalent cobalts (Co^{3+}) are indicated by arrows. Dashed lines represent valence charges and magnetic moments of cations and anions in the defect-free CoO. The vacant site was initially occupied by the Co atom having the fractional coordinates $(\frac{1}{2},\frac{1}{2},\frac{1}{2})$.

balt sublattice having the opposite spin direction. This results in the zero magnetic moment per $Co_{0.93}O$ supercell. Such supercell has now both cationic sublattices equally defected, and the spin-up and spin-down ferromagnetic sublattices of the $Co_{0.93}O$ system are symmetric. The majority-spin component on one cobalt sublattice is the minority-spin component on the other Co sublattice. Therefore, both cation vacancies see the same local environment, albeit with a reversed spin ordering. This leads to a symmetric oxygen band as shown in the lower panel of Fig. 4. No spin polarization of oxygen $2p$ bands is observed now. Both spin channels are identical since they both contribute the same number of states to DOS. Bader charge analysis shows that there are two trivalent cobalt ions in each Co sublattice, i.e., four Co^{3+} per whole supercell containing two V_{Co}. The distance between trivalent cation and the nearest anion decreases to 2.05 Å as compared to the initial Co-O bond length of 2.15 Å. The valence charges of $+1.68e$ and the magnetic moments of $3.16\mu_B$ are found for Co^{3+} ions created as far as 4.29 and 6.04 Å from the vacancy site. The valence charge and the magnetic moment distributions against the distance from the vacancy located in the spin-down Co sublattice are shown in Fig. 5. Both the valence charges and magnetic moments on divalent cobalt ions oscillate around the initial values of $+1.33e$ and $2.74\mu_B$, respectively. Trivalent cobalts introduce their $3d$ states into the band gap and their acceptor levels are situated about 1.5 eV above the valence band maximum. The upper panel in Fig. 4 shows the density of states for the spin-up Co sublattice as the situation looks the same for the other sublattice, although with a reversed spin polarization. Each cation vacancy is accompanied by two trivalent configurations which are, here, also due to the charge-transfer process which converts four divalent cobalts into trivalent ions. Some of the initially localized Co^{2+} states are used to fill up the holes in the oxygen band.

D. Comparison with experiment

Our *ab initio* calculations can be partly compared with the emission Mössbauer spectroscopy experiments[16,29] performed on CoO single crystals doped with radioactive ^{57}Co. The Mössbauer (^{57}Co)CoO source was measured under reduced oxygen partial pressure (10^{-4} atm).[16] Therefore, the low concentration of vacancies (high sample stoichiometry) was assured.

The Mössbauer effect has been often used as a microscopic tool to study the charge states and local environment of dopants in different solids.[30] This is mainly due to the fact that Mössbauer spectroscopy can measure the hyperfine interactions at the position of the resonant nucleus. The hyperfine interactions can be quite generally defined as interactions of the nucleus being in a well defined quantum state (stable or metastable state) with the surrounding medium. These interactions are purely electromagnetic in origin. They are responsible for shifts and splittings of nuclear levels, which can be measured very accurately from the gamma-resonance spectrum. Nuclear electric monopole, electric quadrupole, and magnetic dipole hyperfine interactions are measured by the isomer shift, quadrupole splitting, and the magnetic splitting of the spectrum, respectively. The electron density on the resonant nucleus is affected by the electronic structure of its surrounding, both directly by the s-like valence or conduction electrons and indirectly through changes

in the screening of the core by outer electrons. Since the isomer shift can be related to the difference in the electronic charge density at the source nuclei compared to that at absorber nuclei, it can be useful in inferring the electronic configuration of ions in different environments. The hyperfine interactions of a doped (resonant) atom depend mainly on its local state and its immediate surrounding, hence, the local configurations of impurity ions manifest themselves in different components of the Mössbauer spectra. The isomer shift reflects the local electronic structure of the resonant impurity, and therefore, it is strongly affected by such lattice defects as vacancies or their clusters.

Typical Mössbauer spectra of CoO measured in the vicinity of room temperature consist of two singlets corresponding to Fe^{2+} (ferrous line) and Fe^{3+} (ferric line), both in high-spin configuration.[16] Additionally, a magnetically split component assigned to Fe^{2+} is observed. Single lines represent paramagnetic states, while the hyperfine pattern is due to antiferromagnetic state. The isomer shifts of ferric and ferrous lines are equal, $-0.37(5)$ and $-1.1245(8)$ mm/s, respectively. These shifts are typical for high-spin Fe^{3+} and Fe^{2+} ions. Iron impurities could be considered as isolated ions within the cobalt sublattice since the overall Fe concentration remained very low (40 at. ppm of ^{57}Co and ^{57}Fe altogether). Electron capture decay converts the parent ^{57}Co located substitutionally in the cobalt sublattice either to ferrous or ferric daughter ions. The equilibrium is reached in a short time after the decay, i.e., all aftereffects caused by the radioactive decay vanish, at least within a time window accessible to the Mössbauer effect. The oxidation state of the daughter ion depends on the impurity surrounding. A divalent Fe is born in the almost perfect environment and the charge state of the parent ion remains unchanged ($^{57}Co^{2+}$ transforms directly to $^{57}Fe^{2+}$). Ferrous iron can also be created in the host lattice far away from the vacancy as the very distant defects have no influence on the valence state of iron seen by emission Mössbauer spectroscopy. A divalent state of iron has to be considered as a long-lived metastable state at low temperatures. A different behavior is observed for a daughter impurity created in the lattice disturbed by the vacancies in the neighborhood. Newly born iron located in the vicinity of vacancies transforms rapidly to the high-spin ferric iron ($^{57}Fe^{2+} \rightarrow {}^{57}Fe^{3+} + e^-$). The ferric line is slightly broader than the ferrous line, indicating that ferric ions experience some spurious electric quadrupole interaction due to the lattice and charge distribution caused by defects. It is very unlikely that the direct electron transfer between ferrous and ferric ions takes place as the iron is extremely diluted.

Perfectly stoichiometric phase cannot be made, i.e., cobalt vacancies are always present. Vacancies are believed to stay in the uncharged state in the ground state of the crystal. Therefore, each vacancy has to be accompanied by two Co^{3+} cations in order to maintain charge neutrality. It is also likely that in the vicinity of vacancies and prior to the formation of nucleogenic iron, the charge is transferred from the divalent ^{57}Co to the oxygen band, leaving the parent radioactive impurity in the trivalent state. In such a case, the daughter impurity (the nucleogenic iron) retains the valence state of the parent ion ($^{57}Co^{2+} \rightarrow {}^{57}Co^{3+} + e^-$ and, subsequently, $^{57}Co^{3+} \rightarrow {}^{57}Fe^{3+}$). Hence, the trivalent ions (or impurities) are always present in the CoO lattice decorated with the cationic vacancies and they originate from a charge-transfer process.

Results obtained by emission Mössbauer spectroscopy are indirectly supported by our *ab initio* calculations. Despite the calculations having been performed without taking into account the iron impurities, they resulted in the stable solutions which involved the trivalent ion configurations. On the other hand, atomistic simulations carried out by Grimes and Chen[31] confirm that the CoO lattice is able to accommodate a variety of trivalent cations which are strongly associated with their charge compensating cation vacancies.

IV. CONCLUSIONS

Cation vacancies reduce the effective band gap of CoO via the introduction of acceptor levels. These levels are due to the trivalent cations which are created in the CoO matrix. They result from a partial delocalization of *d* states of divalent cations. Delocalized electrons are transferred to the oxygen band where they compensate the holes created by cation vacancies. Cations which participate in the charge transfer exhibit shorter bonds as compared to the bond lengths of the remaining cations. This facilitates the charge-transfer process. Trivalent ions are created in both ferromagnetic cobalt sublattices so as to retain the antiferromagnetic arrangement of cations. Trivalent cobalts tend to reside in spatially separated lattice sites, i.e., they can be treated as isolated ions within the cation sublattice. The number of delocalized *d* electrons depends on the vacancy concentration, i.e., it increases with increasing nonstoichiometry. The concentration of trivalent cations is twice as large as the concentration of cation vacancies.

The top of the valence band of the cation-deficient CoO is dominated by oxygen $2p$ states which hybridize with cobalt $3d$ states, while the bottom of the conduction band is mainly composed of divalent cobalt $3d$ orbitals.

ACKNOWLEDGMENTS

This work was supported by the Polish Ministry of Scientific Research (MNiSW), Grant No. 3T11F 031 29. Interdisciplinary Modeling Center (ICM), Warsaw University, Poland is acknowledged for providing the computer facilities under Grant No. G28-12.

*Corresponding author; FAX: +48126372243; sfwdowik@cyf-kr.edu.pl

[1] S. Jin, T. H. Tiefel, M. McCormack, R. A. Fastnacht, R. Ramesh, and L. H. Chen, Science **264**, 413 (1994).
[2] A. J. Mills, Nature (London) **392**, 147 (1998).
[3] Y. A. Soh and G. Aeppli, Nature (London) **417**, 392 (2002).
[4] V. I. Anisimov, J. Zaanen, and O. K. Andersen, Phys. Rev. B **44**, 943 (1991).
[5] S. L. Dudarev, G. A. Botton, S. Y. Savrasov, C. J. Humphreys, and A. P. Sutton, Phys. Rev. B **57**, 1505 (1998).
[6] A. Svane and O. Gunnarsson, Phys. Rev. Lett. **65**, 1148 (1990).
[7] Z. Szotek, W. M. Temmerman, and H. Winter, Phys. Rev. B **47**, 4029 (1993).
[8] D. Ködderitzsch, W. Hergert, Z. Szotek, and W. M. Temmerman, Phys. Rev. B **68**, 125114 (2003).
[9] J. B. Goodenough, *Les Oxides des Metaux de transition* (Gautiers-Villars, Paris, 1973).
[10] J. van Elp, J. L. Wieland, H. Eskes, P. Kuiper, G. A. Sawatzky, F. M. F. de Groot, and T. S. Turner, Phys. Rev. B **44**, 6090 (1991).
[11] W. Jauch, M. Reehuis, H. J. Bleif, F. Kubanek, and P. Pattison, Phys. Rev. B **64**, 052102 (2001).
[12] W. Jauch and M. Reehuis, Phys. Rev. B **65**, 125111 (2002).
[13] R. Dieckman, Z. Phys. Chem., Neue Folge **107**, 189 (1977).
[14] P. K. Khowash and D. E. Ellis, Phys. Rev. B **39**, 1908 (1989); **36**, 3394 (1987).
[15] J. Nowotny, I. Sikora, and M. Rekas, J. Electrochem. Soc. **131**, 94 (1984); Oxid. Met. **10**, 311 (1976).
[16] K. Ruebenbauer and U. D. Wdowik, J. Phys. Chem. Solids **65**, 1785 (2004); **65**, 1917 (2004).
[17] C. G. Shull, W. A. Strauser, and O. Wollan, Phys. Rev. **83**, 333 (1951).
[18] W. L. Roth, Phys. Rev. **110**, 1333 (1958).
[19] B. Morosin, Phys. Rev. B **1**, 236 (1970); L. C. Bartel and B. Morosin, *ibid.* **3**, 1039 (1971); B. T. M. Willis and H. P. Rooksby, Acta Crystallogr. **6**, 827 (1953).
[20] D. Herrmann-Ronzaud, P. Barlet, and J. Rossat-Mignod, J. Phys. C **11**, 2123 (1978).
[21] G. A. Sawatzky and J. W. Allen, Phys. Rev. Lett. **53**, 2339 (1984); J. Zaanen, G. A. Sawatzky, and J. W. Allen, *ibid.* **55**, 418 (1985).
[22] G. Kresse and J. Furthmüller, VASP, Vienna, Austria, 1999; Comput. Mater. Sci. **6**, 15 (1996); G. Kresse and J. Hafner, Phys. Rev. B **47**, 558 (1993); G. Kresse and J. Furthmüller, *ibid.* **54**, 11169 (1996).
[23] P. E. Blöchl, Phys. Rev. B **50**, 17953 (1994).
[24] J. P. Perdew, J. A. Chevary, S. H. Vosko, K. A. Jackson, M. R. Pederson, D. J. Singh, and C. Fiolhais, Phys. Rev. B **46**, 6671 (1992).
[25] U. D. Wdowik and K. Parlinski, Phys. Rev. B **75**, 104306 (2007).
[26] H. J. Monkhorst and J. D. Pack, Phys. Rev. B **13**, 5188 (1976).
[27] P. E. Blöchl, O. Jepsen, and O. K. Andersen, Phys. Rev. B **49**, 16223 (1994).
[28] R. Bader, *Atoms in Molecules: A Quantum Theory* (Oxford University Press, New York, 1990); G. Henkelman, A. Arnaldsson, and H. Jónsson, Comput. Mater. Sci. **36**, 254 (2006).
[29] W. R. Helmes and J. G. Mullen, Phys. Rev. B **4**, 750 (1971); C. J. Song and J. G. Mullen, Solid State Commun. **17**, 549 (1975); Phys. Rev. B **14**, 2761 (1976).
[30] N. N. Greenwood and T. C. Gibb, *Mössbauer Spectroscopy* (Chapman and Hall, London, 1971); *Mössbauer Spectroscopy*, edited by U. Gonser (Springer-Verlag, Berlin, 1975).
[31] R. W. Grimes and S. P. Chen, J. Phys. Chem. Solids **61**, 1263 (2000).